Collective Oscillations of an Imbalanced Fermi Gas: Axial Compression Modes and Polaron Effective Mass

Sylvain Nascimbene, Nir Navon, Kaijun Jiang, Leticia Tarruell, Martin Teichmann, Jason Mckeever, Frédéric Chevy, Christophe Salomon

Collective Oscillations of an Imbalanced Fermi Gas: Axial Compression Modes and Polaron Effective Mass

S. Nascimbène[1], N. Navon[1], K. J. Jiang[1], L. Tarruell[2], M. Teichmann[3], J. McKeever[4], F. Chevy[1], and C. Salomon[1]
[1]*Laboratoire Kastler Brossel, CNRS, UPMC, École Normale Supérieure, 24 rue Lhomond, 75231 Paris, France*
[2]*Institute for Quantum Electronics, ETH Zurich, 8093 Zurich, Switzerland*
[3]*Max-Born-Institut, Max-Born-Strasse 2 A, 12489 Berlin, Germany*
[4]*IOS, CQIQC and Dept. of Physics, University of Toronto, Canada*
(Dated: July 16, 2009)

We investigate the low-lying compression modes of a unitary Fermi gas with imbalanced spin populations. For low polarization, the strong coupling between the two spin components leads to a hydrodynamic behavior of the cloud. For large population imbalance we observe a decoupling of the oscillations of the two spin components, giving access to the effective mass of the Fermi polaron, a quasi-particle composed of an impurity dressed by particle-hole pair excitations in a surrounding Fermi sea. We find $m^*/m = 1.17(10)$, in agreement with the most recent theoretical predictions.

PACS numbers: 03.75.Ss; 05.30.Fk; 32.80.Pj; 34.50.-s

The study of the low lying excitation modes of a complex system can be a powerful tool for investigation of its physical properties. For instance, the Earth's structure has been probed using the propagation of seismic waves in the mantle, and the ripples in space-time propagated by gravitational waves can be used as probes of extreme cosmic phenomena. In ultra-cold atomic gases, the measurement of low energy modes of bosonic or fermionic systems has been used to probe superfluidity effects [1], to measure the angular momentum of vortex lattices [2] and to characterize the equation of state of fermionic superfluids [3, 4].

In this paper, we study the excitation spectrum of an ultra-cold Fermi gas with imbalanced spin populations. This topic was initiated in the 60's by the seminal works of Clogston and Chandrasekhar [5, 6] and found only recently an experimental confirmation thanks to the latest developments in ultra-cold Fermi gases [7, 8]. These dramatic experiments have observed that when a fermionic superfluid is polarized through imbalance of spin populations, the trapped atomic cloud forms a shell structure. The energy gap associated with pairing maintains a superfluid core where the two spin densities are equal, while the outer shell is composed by a normal gas with imbalanced spin densities (see Fig.1). Here, we extend this work to the dynamical properties of these systems and we focus on the regime of strong interactions, where the scattering length a is infinite. We show in particular that the study of the axial breathing mode provides valuable insight on the dynamical properties of a quasi-particle, the Fermi polaron, that was introduced recently to describe the normal component occupying the outer shell of the cloud [9, 10, 11, 12, 13, 14]. The Fermi polaron is composed of an impurity (labelled 2) immersed in a non-interacting Fermi sea (labelled 1), and is analogous to the polaron of condensed matter physics, *i.e.* an electron immersed in a bath of non-interacting (bosonic) phonons. According to the Landau theory of the Fermi liquid, the low energy spectrum of the polaron is similar to that of a free particle and can, in the local density approximation (LDA), be recast as

$$E_2(\boldsymbol{r},\boldsymbol{p}) = AE_{F1}(\boldsymbol{r}) + V(\boldsymbol{r}) + \frac{p^2}{2m^*} + ... \qquad (1)$$

where V is the trapping potential, $E_{F1}(\boldsymbol{r}) = E_{F1}(\boldsymbol{0}) - V(\boldsymbol{r})$ is the local Fermi energy of the majority species, A is a dimensionless quantity characterizing the attraction of the impurity by the majority atoms and m^* is the effective mass of the Fermi polaron. For $a = \infty$, $A = -0.61$ has been determined both experimentally [14] and theoretically [9, 10, 11, 12, 13], while slight disagreements still exist on the value of the effective mass. Fixed node Monte-Carlo suggests $m^*/m = 1.09(2)$ [15], systematic diagrammatic expansion yields $m^*/m = 1.20$ [11] and analysis of density profiles (such as Fig.1) gives $m^*/m = 1.06$ [16].

From Eq. (1), the quasi-particle evolves in an effective potential $V^*(\boldsymbol{r}) = (1 - A)V(\boldsymbol{r})$. Assuming $V(\boldsymbol{r})$ to be harmonic with frequency ω, the polaron is trapped in an effective potential of frequency ω^* [9]:

$$\frac{\omega^*}{\omega} = \sqrt{\frac{1-A}{m^*/m}}. \qquad (2)$$

In this paper we determine the effective mass through the measurement of the oscillation frequency ω^* in the axial direction (labelled z) of a cylindrically symmetric trap.

Our experimental setup is an upgraded version of the one presented in [17]. 7×10^6 ^{6}Li atoms in the hyperfine state $|F = 3/2, m_F = +3/2\rangle$ are loaded into a mixed magnetic/optical trap at 100 μK. The optical trap uses a single beam of waist $w_0 = 35$ μm and maximum power $P = 60$ W operating at a wavelength $\lambda = 1073$ nm. The atoms are transferred into the hyperfine ground state $|1/2, 1/2\rangle$, and a spin mixture is created by a radio-frequency sweep across the hyperfine transition $|1/2, 1/2\rangle \rightarrow |1/2, -1/2\rangle$. By varying the rate of

this sweep, we control the sample's degree of polarization $P \equiv (N_1 - N_2)/(N_1 + N_2)$, where N_1 (resp. N_2) is the atom number of the majority (resp. minority) spin species. The mixture is then evaporatively cooled in 6 s by reducing the laser power to 70 mW. This is done at a magnetic field $B = 834$ G, which corresponds to the position of the broad Feshbach resonance in ^{6}Li where the scattering length is infinite and where further experiments are performed. Typical radial frequencies are $\omega_x = \omega_y \sim 2\pi \times 400$ Hz. The axial confinement of the dipole trap is enhanced by the addition of a magnetic curvature, leading to an axial frequency $\omega_z \sim 2\pi \times 30$ Hz. Our samples contain $\sim 8\times10^4$ atoms in the majority spin state at a temperature $T \lesssim 0.09\ T_F$. The temperature is evaluated by fitting the wings of the majority density profile outside the minority radius. In this region, the gas is non-interacting, allowing unambiguous thermometry of the inner, strongly-interacting part of the cloud [18]. Here, T_F is defined as the Fermi temperature of an ideal gas whose density profile overlaps the majority one in the fully polarized rim. Our thermometry's precision is limited by the finite signal to noise ratio of the data, hence the quoted upper bound.

The two spin states are imaged sequentially using *in situ* absorption imaging. To prevent heating from the scattered photons and the strong interactions between the two species, the duration of the two imaging pulses as well as their separation must be short (10 μs each in our case). By reversing the order in which we image the two spin components, we checked that the imaging of the first species did not significantly influence the second. Typical integrated density profiles of the atom cloud $\bar{n}(z) = \int \mathrm{d}x\mathrm{d}y\ n(x,y,z)$, where $n(x,y,z)$ is the 3D atom density, are presented in Fig.1. These profiles display the characteristic features already observed by the MIT group [18]: a flat-top structure in the superfluid region confirming the existence of a fully paired core satisfying the LDA [19], an intermediate phase where the two spin species are present with unequal densities, and an outer rim containing only majority atoms. Following [20], we compare our density profiles to the prediction for the equation of state of the different phases and find fairly good agreement. In particular, we observe that the superfluid core disappears for polarizations $P > 0.76(3)$. This limit agrees well with the measurement of the MIT group [8] and differs from the Rice group value [7].

We excite the axial breathing mode by switching off the axial magnetic trapping field for 1 ms. The effect of this excitation is twofold: in addition to nearly suppressing the axial confinement, the bias field is increased up to 1050 G, where $k_F a \sim -1$, so that the gas is no longer strongly interacting. This scheme provides a spatially selective excitation of the cloud. Indeed, while the reduction of the trapping frequency perturbs the whole cloud, the modification of the scattering length only acts in the region where the two spin components overlap. In the regime of strong polarization, these two regions are well separated, leading to a differential excitation of the two spin components.

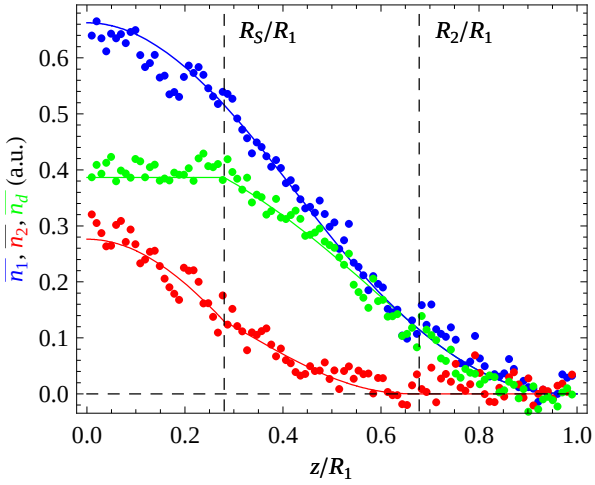

FIG. 1: (color online) Integrated density profiles of an imbalanced Fermi gas. Blue: majority atoms $\bar{n}_1(z)$; Red: minority atoms $\bar{n}_2(z)$; Green: difference $\bar{n}_d = \bar{n}_1 - \bar{n}_2$. In this latter case, the flat-top feature signals a cancellation of the density difference at the center of the trap, characteristic of the existence of a fully paired superfluid core. The superfluid (resp. minority) radius R_S (resp. R_2) are marked by vertical dashed lines. The full color lines correspond to the prediction of Monte-Carlo theories [20], the only fit parameters being the number of atoms in each spin state, $N_1 = 8.0 \times 10^4$, $N_2 = 2.4 \times 10^4$ for this image. The axial (radial) trap frequency is 18.6 Hz (420 Hz).

Let us first focus on the oscillations of the majority spin species presented in Fig.2. Typical dynamics of the outer radius $R_1(t)$ of the majority component are exemplified by Fig.2a. For each polarization, this time evolution is fitted using an exponentially damped sinusoid, with $R_1(t) = R_1^{(0)}(1+A_1\cos(\omega_1 t+\varphi)e^{-\gamma_1 t})$, and the variations of ω_1 and γ_1 as a function of P are displayed in Fig.2b and Fig.2c. One remarkable feature of this graph is the frequency plateau for polarizations $P \lesssim 0.7$, corresponding approximately to the domain where a superfluid core is present in the cloud. Although in this range of parameters, the dynamics of the system is fairly complex due to the strong coupling between the superfluid and normal components, a simple argument based on a sum rule approach generalizing the result of [21] allows us to understand this property.

We describe the system by the Hamiltonian $H = \sum_i p_i^2/2m + U(\boldsymbol{r}_1, \boldsymbol{r}_2, ...)$, where $\boldsymbol{r}_i$ (resp. $\boldsymbol{p}_i$) is the position (resp. momentum of particle i), m is the mass of the atoms and U includes both trapping potential and interatomic interaction. The compression of the trapping frequency in the z direction is associated with the operator $F = \sum_i z_i^2$. Let us introduce the moments of the

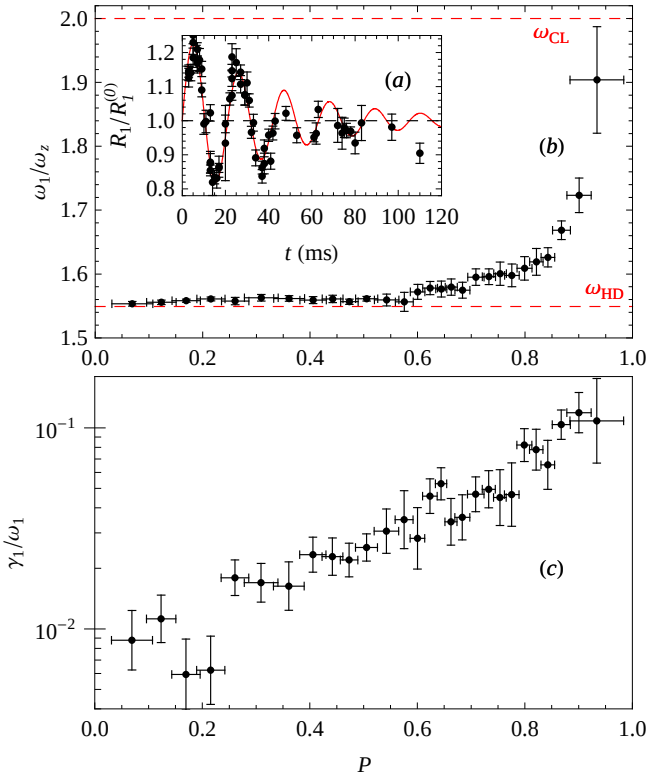

FIG. 2: (a) Oscillations of the axial radius of the majority component, for a population imbalance $P = 0.85(2)$, beyond the Clogston limit. The full line corresponds to a fit by an exponentially damped sinusoid. (b) Frequency of the breathing mode ω_1 normalized to the axial trapping frequency ω_z. The superfluid (resp. collisionless) limits $\omega_1 = \sqrt{12/5}\,\omega_z$ (resp. $2\,\omega_z$) are indicated by the red lines. The axial (radial) trap frequency is 28.9(1) Hz (420 Hz). (c) Damping rate γ_1 as the function of polarization (in log scale). Note that our data are limited to $P < 0.95$ due to the small minority atom number ($N_2 \lesssim 2 \times 10^3$) at such high polarizations.

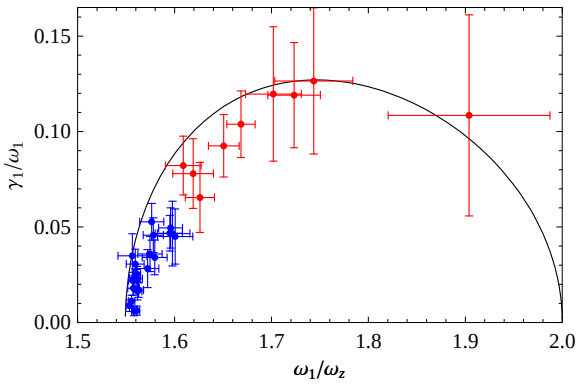

FIG. 3: Comparison of our experimental results with the parametric curve $(\omega_1(\tau)/\omega_z, \gamma_1(\tau)/\omega_1(\tau))$ deduced from prediction (4). The data in blue (red) correspond to polarizations $P < 0.8$ ($P > 0.8$).

spectral distribution associated with F and defined by

$$m_k = \sum_{n\neq 0} (E_n - E_0)^k \, |\langle 0|F|n\rangle|^2 \,,$$

where the $|n\rangle$ are the eigenstates of H associated with the eigenvalue E_n, and $|0\rangle$ is the many-body ground state. We assume that the operator F mainly couples $|0\rangle$ to one excited state $|1\rangle$. In this case, the frequency of the breathing mode excited by the axial compression of the trap is given by $\omega_1 = (E_1 - E_0)/\hbar \simeq \sqrt{m_1/m_{-1}}/\hbar$. An explicit calculation of these two moments leads to the following expression :

$$\omega_1^2 \simeq -2\langle z^2\rangle \Big/ \frac{\partial\langle z^2\rangle}{\partial\omega_z^2} \,. \qquad (3)$$

For a unitary gas, LDA imposes that the mean radius of the cloud is given by $\langle z^2\rangle = R_{TF}^2 f(P)$, where R_{TF} is the radius of an ideal Fermi gas in the same trap and with the same atom number and f is some universal function of the polarization [22]. Using this assumption, the calculation of the oscillation frequency is straightforward and yields $\sqrt{\frac{12}{5}}\omega_z = 1.55\omega_z$, *i.e.* the hydrodynamic prediction [3, 23] for $P = 0$, *regardless of the polarization of the sample*. This argument is in good agreement with our experimental findings (Fig.2b).

At larger polarizations the frequency sharply increases towards the collisionless value. The damping rate, very small in the balanced superfluid, increases by a factor ~ 20 for higher imbalances [24]. Interestingly, as seen in Fig.3, this behavior is consistent with a general argument about relaxation processes in fluid dynamics [25]. Indeed, one can relate ω_1 and γ_1 through

$$\omega^2 = \omega_{CL}^2 + \frac{\omega_{HD}^2 - \omega_{CL}^2}{1 + i\omega\tau}, \qquad (4)$$

where $\omega = \omega_1 + i\gamma_1$, $\omega_{HD} = \sqrt{12/5}\,\omega_z$ (resp. $\omega_{CL} = 2\,\omega_z$) is the hydrodynamic (resp. collisionless) frequency and τ is an effective relaxation rate.

Measurements of ω_1/ω_z in three different traps of aspect ratios 8.2, 9.0 and 14.5 give identical results (within 3%) for all polarizations. By contrast, the effect of temperature is more pronounced. At $0.12(1)\,T_F$, $\omega_1(P)$ remains equal to the hydrodynamic prediction at all attainable polarizations with $P_{max} = 0.95$, for a cloud of $N_1 \sim 2 \times 10^5$ majority atoms held in a trap of aspect ratio 22. This illustrates the role of Pauli blocking at the lowest temperatures which favors collisionless behavior.

Let us now consider the dynamics of the minority cloud (we recall that subscript 2 refers to the impurity atoms). We observe that for polarizations smaller than $P \sim 0.75$, the oscillation frequencies and damping rates of the two spin species are equal, indicating a strong coupling between them. By contrast, for $P > 0.75$, a Fourier spectrum of $R_2(t)$ reveals two frequencies (Fig.4a). The lower frequency ω_{2a} is equal to the majority oscillation fre-

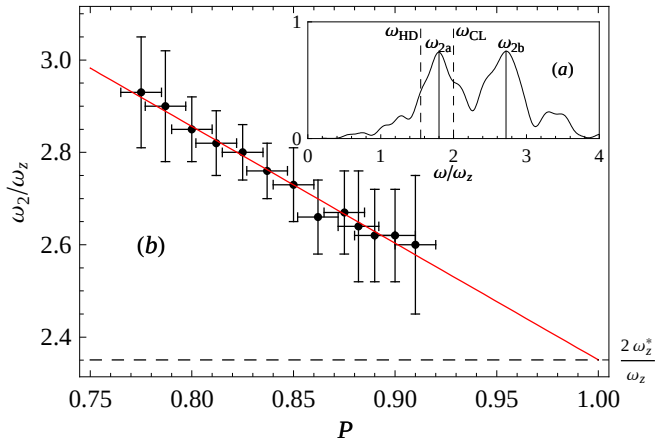

FIG. 4: (a) Frequency power spectrum for $P = 0.90(2)$. The peak between $\omega_{\rm HD}$ and $\omega_{\rm CL}$ corresponds to the oscillation in phase with the majority, the other one to the polaron oscillation. (b) Frequency of the polaron component as a function of polarization. All frequencies are normalized to ω_z.

quency ω_1. We interpret the higher frequency ω_{2b}, whose weight increases with polarization, as the axial breathing of the minority atoms out of phase with the majority cloud. A linear extrapolation of this frequency to $P = 1$ gives the oscillation frequency of a dilute gas of weakly interacting polarons inside a Fermi sea at rest, $\omega_{2b}(P \to 1) = 2.35(10)\omega_z$ (Fig.4b). The uncertainty represents the standard deviation of a linear fit taking into account the statistical uncertainties of the ω_{2b} measurements for each polarization.

By identifying the breathing mode frequency ω_{2b} as $2\omega_z^*$ and using (2), we deduce the mass of the quasiparticle : $m^*/m = 1.17(10)$. This is the first dynamic measurement of the polaron effective mass, in good agreement with the most recent theoretical predictions [11, 26], and with static observations [16, 20]. m^* is close to m (albeit different), a surprising feature for a strongly interacting system at unitarity. We also exclude a mass $m^* = 2m$ that one would expect for a deeply bound bosonic molecule.

In conclusion, we have studied the low frequency breathing modes of an elongated Fermi gas with imbalanced spin populations. In the presence of a superfluid core, the majority and minority components oscillate in phase with a frequency that is largely independent of the spin polarization and in agreement with the hydrodynamic prediction. At strong polarizations, the minority atom oscillation reveals a second frequency, that we interpret as the Fermi polaron breathing mode. Further investigations will extend our work to all values of the scattering length. In particular, they should provide a clear signature of the polaron-molecule transition [14, 27]. The role of interactions between polarons and damping phenomena should also be clarified [28].

We are grateful to S. Stringari, A. Recati, C. Lobo, M. Zwierlein, J. Dalibard and Y. Castin for fruitful discussions as well as K. Magalhães and G. Duffy for experimental support. We acknowledge support from ESF (FerMix), SCALA, ANR FABIOLA, Région Ile de France (IFRAF), ERC and Institut Universitaire de France.

[1] S. Giorgini, L. Pitaevskii, and S. Stringari, Rev. Mod. Phys. **80**, 1215 (2008).
[2] F. Chevy, K. W. Madison, and J. Dalibard, Phys. Rev. Lett. **85**, 2223 (2000).
[3] M. Bartenstein, A. Altmeyer, S. Riedl, S. Jochim, C. Chin, J. Denschlag, and R. Grimm, Phys. Rev. Lett. **92**, 203201 (2004).
[4] J. Kinast, S. Hemmer, M. Gehm, A. Turlapov, and J. Thomas, Phys. Rev. Lett. **92**, 150402 (2004).
[5] A. Clogston, Phys. Rev. Lett. **9**, 266 (1962).
[6] B. S. Chandrasekhar, App. Phys. Lett. **1**, 7 (1962).
[7] G. Partridge, W. Li, R. Kamar, Y. Liao, and R. Hulet, Science **311**, 503 (2006).
[8] M. Zwierlein, A. Schirotzek, C. Schunck, and W. Ketterle, Science **311**, 492 (2006).
[9] C. Lobo, A. Recati, S. Giorgini, and S. Stringari, Phys. Rev. Lett. **97**, 200403 (2006).
[10] F. Chevy, Phys. Rev. A **74**, 063628 (2006).
[11] R. Combescot and S. Giraud, Phys. Rev. Lett. **101**, 050404 (2008).
[12] R. Combescot, A. Recati, C. Lobo, and F. Chevy, Phys. Rev. Lett. **98**, 180402 (2007).
[13] N. Prokof'ev and B. Svistunov, Phys. Rev. B **77**, 125101 (2008).
[14] A. Schirotzek, C.-H. Wu, A. Sommer, and M. W. Zwierlein, Phys. Rev. Lett. **102**, 230402 (2009).
[15] S. Pilati and S. Giorgini, Phys. Rev. Lett. **100**, 030401 (2008).
[16] Y. Shin, Phys. Rev. A **77**, 041603 (2008).
[17] T. Bourdel, L. Khaykovich, J. Cubizolles, J. Zhang, F. Chevy, M. Teichmann, L. Tarruell, S. Kokkelmans, and C. Salomon, Phys. Rev. Lett. **93**, 050401 (2004).
[18] Y. Shin, C. Schunck, A. Schirotzek, and W. Ketterle, Nature **451**, 689 (2008).
[19] T. De Silva and E. Mueller, Phys. Rev. Lett. **97**, 070402 (2006).
[20] A. Recati, C. Lobo, and S. Stringari, Phys. Rev. A **78**, 023633 (2008).
[21] L. Vichi and S. Stringari, Phys. Rev. A **60**, 4734 (1999).
[22] F. Chevy, Phys. Rev. Lett. **96**, 130401 (2006).
[23] M. Amoruso, I. Meccoli, A. Minguzzi, and M. Tosi, Eur. Phys. J. D. **7**, 441 (1999).
[24] The damping rate is expected to vanish in the truly collisionless limit, a regime difficult to access experimentally.
[25] L. Landau and E. Lifshitz, Course of Theoretical Physics Vol. 6 : Fluid Mechanics (1987).
[26] S. Pilati and S. Giorgini, Phys. Rev. Lett. **100**, 30401 (2008).
[27] N. Prokof'ev and B. Svistunov, Phys. Rev. B **77**, 020408 (2008).
[28] G. Bruun, A. Recati, C. Pethick, H. Smith, and S. Stringari, Phys. Rev. Lett. **100**, 240406 (2008).